tive and chronic inflammatory status, the significant interrelationships among obesity-related indices, oxidative stress, inflammatory markers and adipokines have been well documented [10, 11, 13-15]. However, most of the studies just examined the indirect anthropometric indices such as BMI and WC as well as their relationships with systemic oxidative stress [10, 11, 15], or focused on the association between certain regional adiposity (abdomen) and oxidative stress without taking total body FM and pattern of distribution into consideration [12, 16]. Because adipose tissue accumulating in different anatomic compartments (regional adiposity) may have unique characteristics related to different expression of enzymes and receptors involving in triglyceride synthesis [17], lipolysis [18] and adipokine synthesis [18], and lines of evidence also suggested that different regional adiposity have different clinical implications [19], for instance, abdominal (central) adiposity is closely related with high CVD risks [2] whereas lower-body (peripheral) adiposity is reported to relate with a favorable lipid profile against the adverse effects of obesity [19-22]. Therefore it is essential to exam the relationship between regional adiposity and oxidative stress, and to further identify the role of oxidative stress in mediating metabolic effects of regional adiposity. Until now regional adiposity and its correlation with systemic oxidative stress has not been well documented.

In the present study, cross-sectional study was conducted in a middle-aged clinically healthy female cohort. Systemic oxidative stress was evaluated by urinary creatinine-indexed 8-epi-prostaglandin $F_{2\alpha}$ (8-epi-$PGF_{2\alpha}$), a validated biomarker of oxidative stress [23]. Body fat mass distribution was examined by dual-energy X-ray absorptiometry (DXA). Their relationships with obesity-related metabolic characteristics, including inflammatory markers, adipokines, and lipid profile were investigated. Men and women have different FM distribution pattern. FM tends to depot in the abdominal/central region in men whereas women tend to accumulate FM in the lower-body/peripheral region [24]. Substantial evidence has demonstrated that sex-differences in the FM distribution may lead to distinct metabolic outcomes [25], therefore this study we only included women as subjects in order to keep the confounding factors as low as possible.

Materials and Methods

Subjects

148 middle-aged (39-60 years) clinically healthy women participated in this study. There were 137 (92.6%) pre-menopause and 11 (7.4%) post-menopause women. Subjects with clinical diagnosed endocrine, cardiovascular, hepatic, renal diseases, hormonal contraception or replacement, cigarette smokers and alcohol consuming ≥40g/day were excluded. Nobody received any medications or antioxidative vitamins. The study was approved by the Ethics Committees of Mukogawa Women's University and written informed consents were obtained from all participants.

Anthropometry, body composition and fat mass distribution

Body weight, height, WC were measured following standard procedures and BMI was calculated. DXA with a scanner (Hologic QDR-2000, software version 7.20D, Bedford, MA) was applied to measure body mass distribution. This method uses a three-compartments model of body mass and provides an estimate of regional fat mass (FM), lean tissue and bone mineral. A scanned image of the whole body was divided into six subdivisions: head, trunk, left and right arms and lower-body (Fig. 1). The dividing borders between those subregions were differentiated by a line underneath the chin, a line between the humerus head and the glenoid fossa, and a line at the femoral neck. The trunk region included the chest and abdomen, excluding the pelvis. The lower-body region included the entire hip, thigh, and leg [25]. Regional FM ratios (%FM) were expressed as percentage of regional fat tissue weight/regional body weight×100%. DXA is considered to be the gold standard for determination of body fat and pattern of distribution with lower radiation exposure and less time-consuming compared with computer tomography (CT) scan [26, 27] .

Insulin, glucose, and insulin resistance

Blood samples were obtained in the morning after 12-hr overnight fast. Insulin resistance determined by homeostasis model assessment (HOMA-IR) were calculated using fasting plasma glucose and insulin levels [28].

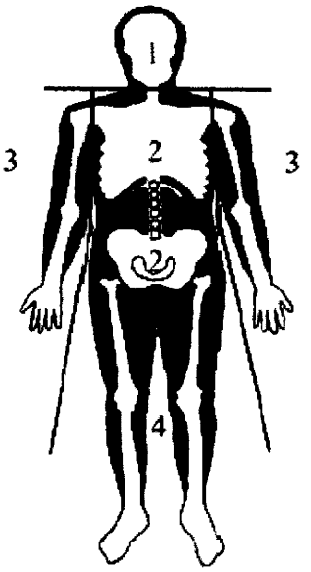

Fig. 1. Standard regions of a dual-energy X-ray absorptiometry scan 1, head; 2, trunk; 3, arms; 4, lower-body

Plasma lipids, lipoprotein, and Apo measurements

Serum lipids [triglycerides (TG), total cholesterol (TC), high-density lipoprotein cholesterol (HDL-C)] were measured using an autoanalyzer (AU5232, Olympus, Tokyo, Japan). Apolipoprotein A-1 (ApoA1), and apolipoprotein B-100 (ApoB) were measured by respective commercially available kits using an Olympus autoanalyzer (AU600, Mitsubishi Chemicals, Tokyo, Japan). Low-density lipoprotein cholesterol (LDL-C) was determined using the Friedewald formula [29]. Small density LDL-C (sd LDL) was measured by a precipitation method described elsewhere [30].

Oxidative stress, adipokines, and inflammatory markers

Urinary 8-epi-$PGF_{2\alpha}$ was measured in the first-voided morning urine sample with an enzyme-liked immunosorbent assay (8-Isoprostane EIA kit, Cayman, Ann Arbor, MI). Intra- and inter- assay CV were 7.5% and 9.2%, respectively. Urinary 8-epi-$PGF_{2\alpha}$ was indexed to creatinine as picograms per milligram creatinine. Adiponectin was assayed by a sandwich enzyme-linked immunosorbent assay (Otsuka Pharmaceutical Co., Ltd., Tokushima City, Japan). Intra- and inter-assay CV were 3.3% and 7.5%, respectively. Leptin were assessed by a RIA kit from LINCO research (St. Charles, MO, interassay CV=4.9%). Highly sensitive C-reactive protein (hsCRP) was measured by an immunoturbidometric assay with the use of reagents and calibrators from Dade Behring Marbura GmbH (Marburg, Germany; interassay CV<5.0%). TNF-α were measured by immunoassays (R&D Systems, Inc., Minneapolis, MN, interassay CV = 6.0%). PAI-1 was measured by an ELISA method (Mitsubishi Chemicals, interassay CV= 8.1 %). For statistical analysis, serum concentrations of hsCRP and TNF-α below the limit of detection were assigned a value of 50μg/liter and 50pg/mL (the lowest limit of detection), respectively.

Statistics

Data were presented as mean±SD. Due to deviation from normal distribution, hsCRP was logarithmic transformed for analysis. Means differences among groups were compared by nonparametric Mann-Whitney U test or ANOVA with Bonferroni correction for multiple comparisons. Univariate correlations of urinary 8-epi-$PGF_{2\alpha}$ with regional FM distribution, and other metabolic parameters were evaluate with both Spearman's rank order and Pearson correlation coefficients. Both methods gave practical identical results, and only Spearman's coefficients were reported here. Stepwise multiple regression analyses were performed to further indentify the most significant variables contributing to the variation of 8-epi-$PGF_{2\alpha}$. All the variables with significant associations with 8-epi-$PGF_{2\alpha}$ in univariate analyses were entered into the model simultaneously. In each following step, the variable having the least significant P value was excluded from the model. Finally, all variables with $P<0.05$ remained in the model. Standardized ß-estimate was used to determine which variable had the strongest effect on 8-epi-$PGF_{2\alpha}$. A two-tailed $P<0.05$ was considered statistically significant. All calculations were performed with SPSS system 15.0 (SPSS Inc, Chicago, IL).

Results

According to the Asian-Pacific redefining criteria of obesity [31], there were 106 normal weight (BMI<23kg/m^2) and 42 over weight (BMI≥23kg/m^2) subjects and nobody could be classified as MetS according to NCEP ATP III [32], IDF [33], or Japanese

Table 1. Anthropometric and metabolic characteristics of the subjects

	Normal weight (n=102)	Over weight (n=46)	*P* value
Age (year)	49.7±3.6	50.0±3.7	0.914
BMI (kg/m^2)	20.4±1.5	25.4±2.0	<0.001
Waist circumeference (cm)	75.1±5.7	86.6±6.9	<0.001
Total FM (kg)	13.435±4.184	21.957±4.967	<0.001
%Total FM	27.3±6.2	36.4±5.2	<0.001
Trunk FM (kg)	7.066±2.502	12.276±2.855	<0.001
%Trunk FM	29.4±7.5	40.4±5.7	<0.001
Arm FM(kg)	1.189±0.536	2.117±0.64	<0.001
%Arm FM	24.8±8.1	34.4±6.1	<0.001
Lower- Body FM (kg)	4.606±1.361	6.809±1.881	<0.001
%Lower- Body FM	28.2±5.9	34.9±6.1	<0.001
HbA_{1C} (%)	5.0±0.3	5.3±0.6	<0.001
HOMA-IR	1.03±0.57	1.61±0.83	<0.001
Triglyceride (mmol/L)	0.85±0.35	1.06±0.48	0.011
Total Cholesterol (mmol/L)	5.79±0.89	5.77±0.92	0.969
HDL Cholesterol (mmol/L)	2.09±0.38	1.80±0.41	<0.001
LDL Cholesterol (mmol/L)	3.31±0.74	3.48±0.82	0.255
sd LDL (mg/dL)	15.15±8.23	22.55±10.11	<0.001
ApoA1 (mg/dL)	182.0±21.3	168.6±21.5	0.001
ApoB (mg/dL)	89.7±18.3	99.3±20.0	0.003
Leptin (ng/mL)	5.9±3.1	11.3±6.0	<0.001
Adiponectin (μg/mL)	12.6±5.2	10.1±3.9	0.004
PAI-1 (ng/mL)	19.5±11.2	33.7±17.7	<0.001
LogCRP	1.28±0.49	1.71±0.49	<0.001
TNF-α (pg/mL)	0.75±0.32	0.83±0.49	0.413
sBP (mmHg)	116.2±11.6	131.7±18.0	<0.001
dBP (mmHg)	71.3±9.1	78.5±12.5	0.001
8-epi-$PGF_{2\alpha}$ (pg/mg.creatinine)	338.6±133.7	430.4±258.3	0.008

Data are the means±SD.BMI, body mass index; FM, fat mss; HOMA-IR, homeostasis model assessment of insulin resistance; sBP, systolic blood pressure; dBP, diastolic blood pressure; sd LDL, small density LDL.

criteria [34]. Their anthropometric and metabolic characteristics were presented in Table 1. Over weight subjects showed higher both indirect anthropometric measurements (BMI, WC) and direct anthropometric measurements (DXA-indices), all the $P<0.001$. For lipid profile, TG, HDL-cholesterol, sd LDL, ApoA1 and ApoB were difference between two groups. HOMA-IR was significantly higher in over weight than normal weight ($P<0.001$). For adipokines and inflammatory markers, leptin, adiponectin, Log (hsCRP), PAI-1 were significantly different between two groups. Urinary 8-epi-$PGF_{2\alpha}$ excretion of over weight subjects was ~ 30% higher than that of normal weight women ($P=0.002$). We also used 25kg/m^2 as BMI cutoff point to divide total subjects into normal weight and over weight group, and the comparisons gave the approximatively identical results (data not shown).

In the univariate correlation analyses (Table 2), 8-epi-$PGF_{2\alpha}$ correlated with all anthropometric parameters, systolic BP and diastolic BP. Among them, the strongest correlations were found among 8-epi-$PGF_{2\alpha}$, lower-body FM, total FM and trunk FM (r=0.353, 0.295, and 0.263, all the $P<0.001$, Fig.2A, 2B, 2C). For metabolic parameters, 8-epi-$PGF_{2\alpha}$ had significant correlations with PAI-1 (r=0.237, $P<0.05$), [Log (hsCRP), r=0.164, $P<0.05$], leptin (r=0.175, $P<0.05$). According to the body FM content (%total FM), 148 women were stratified into high (≥30%, n=72) and

Table 2. Characteristics of all subjects and correlation coefficients with 8-epi-PGF2α

Total subjetcs (n=148)	Mean±SD	r	*P* value
Age (year)	49.8±3.6	0.056	0.499
BMI (kg/m^2)	22.0±2.8	0.238	0.004
Waist circumeference (cm)	78.7±8.1	0.230	0.009
Total FM (kg)	16.062±5.929	0.295	<0.001
%Total FM	30.1±7.3	0.290	<0.001
Trunk FM (kg)	8.672±3.552	0.263	0.001
%Trunk FM	32.9±8.7	0.246	0.003
Arm FM (kg)	1.475±0.712	0.250	0.002
%Arm FM	27.8±8.8	0.254	0.002
Lower-Body FM (kg)	5.285±1.842	0.353	<0.001
%Lower- Body FM	30.3±6.7	0.342	<0.001
HbA_{1c}(%)	5.1±0.4	0.100	0.225
HOMA-IR	1.21±0.71	0.088	0.288
Triglyceride (mmol/L)	0.92±0.4	-0.029	0.725
Total Cholesterol (mmol/L)	5.78±0.9	-0.122	0.138
HDL Cholesterol (mmol/L)	2.00±0.41	-0.036	0.66
LDL Cholesterol (mmol/L)	3.37±0.77	-0.146	0.077
sd LDL (mg/dL)	17.48±9.47	-0.141	0.14
ApoA1 (mg/dL)	177.9±22.2	-0.014	0.867
ApoB (mg/dL)	92.7±19.3	-0.087	0.292
Leptin (ng/mL)	7.6±4.9	0.175	0.033
Adiponectin (μg/mL)	11.8±4.9	0.083	0.314
PAI-1 (ng/mL)	23.9±15	0.237	0.018
LogCRP	1.41±0.53	0.164	0.021
TNF-α (pg/mL)	0.77±0.38	0.047	0.569
sBP (mmHg)	120.0±15.6	0.199	0.015
dBP (mmHg)	73.5±10.8	0.149	0.041
8-epi-$PGF_{2\alpha}$ (pg/mg.creatinine)	367.1±185.8		

Data are the means±SD.BMI, body mass index; FM, fat mss; HOMA-IR, homeostasis model assessment of insulin resistance; sBP, systolic blood pressure; dBP, diastolic blood pressure; sd LDL, small density LDL.

normal (<30%, n=76) subgroups. Significant correlations between lower-body FM and urinary 8-epi-$PGF_{2\alpha}$ excretion were observed in both two groups (for high FM content group, r=0.224, *P*=0.048; for normal FM content group, r=0.315, *P*=0.007).

Because there were strong interrelationships between BMI, WC and DXA indices, all the univariate analyses were repeated after adjustment for BMI and WC. After this correction, the following parameters retained significant correlations with 8-epi-$PGF_{2\alpha}$: lower-body FM (partial r=0.262 *P*=0.004), total FM (partial r=0.218 *P*=0.018) and PAI-1 (partial r=0.208 *P*=0.024). Associations between 8-epi-$PGF_{2\alpha}$ and BMI, WC were disappeared after adjustment for DXA-derived total FM.

The stepwise regression analysis revealed that 11.2% variance of in 8-epi-$PGF_{2\alpha}$ in all study subjects was predicted by lower-body FM and PAI-1 (Table 3). Lower-body FM was the first variable accepted in the model, which account for 8.4% of the variance of 8-epi-$PGF_{2\alpha}$. PAI-1 was the second variable accepted in the model, which contribute 5.0% variance of 8-epi-$PGF_{2\alpha}$ independently.

We compared the urinary 8-epi-$PGF_{2\alpha}$ levels divided by tertile of trunk FM and WC, two surrogate indices for visceral fat accumulation. Among all subjects, 8-epi-$PGF_{2\alpha}$ were significantly increased across the low, middle and high categories of trunk FM

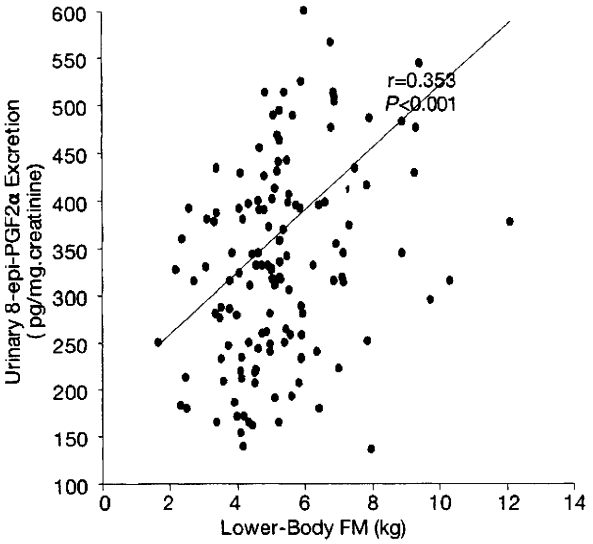

Fig. 2A. Relationship between lower-body fat mass (FM)and urinary 8-epi-$PGF_{2\alpha}$

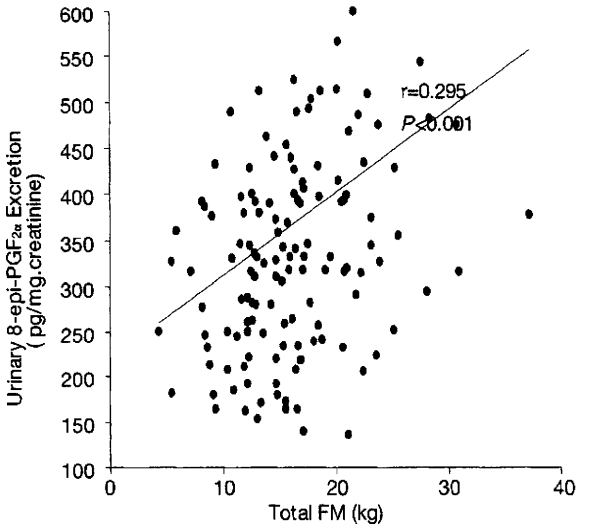

Fig 2B Relationship between total fat mass (FM) and urinary 8-epi-$PGF_{2\alpha}$

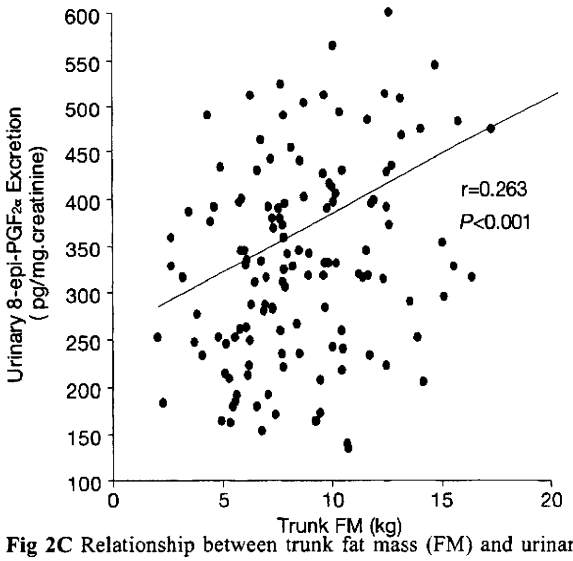

Fig 2C Relationship between trunk fat mass (FM) and urinary 8-epi-$PGF_{2\alpha}$

(for trunk FM category: 334.6±158.0, 346.8±115.3, 424.2±253.0, *P* for trend <0.01) and WC (for WC category: 334.6±135.8, 337.3±129.0, 428.1±252.0, *P* for trend <0.01). Finally, by using Japanese criteria [34] the subjects were divided into 3 groups according to their components of MetS: with 0 risk factor (n=81), 1 risk factor (n=37) and ≥2 risk factors (n=30). Urinary 8-epi-$PGF_{2\alpha}$ excretion were significantly higher in 2 or more risk factors group than 0 and 1 risk factor groups (460.0±204.1 *vs* 337.8±135.9, 355.9±127.1, *P*=0.002 and 0.020, respectively).

Table 3. Multiple regression analysis for estimation of 8-epi-PGF2α in 148 healthy middle-aged women.

Independent variables	standard β coefficients	Adjusted R^2	*P* value
constant	174		<0.001
lower-body FM	0.258	0.084	0.002
PAI-1	0.190	0.112	0.019

n=148, This model includes all the variables which have significant association with 8-epi-$PGF_{2\alpha}$ in Table 2.

Discussion

Oxidative stress is recognized to be a prominent feature of CVD [5, 6] and MetS [16, 35]. The measurement of F2-isoprostane is the most reliable approach to estimate oxidative stress status and lipid peroxidation *in vivo* [26]. In the present study, we demonstrated that all the DXA-derived fat mass indices have positive relationships with systemic oxidative stress in healthy middle-aged women. Furthermore, the observations that subjects with higher trunk FM, WC and more number of MetS components also had higher 8-epi levels suggest the close relationship between oxidative stress and MetS. Our findings not only confirm the previous studies that oxidative stress is correlated with indirect body fat mass measures

(BMI and WC), but also provide evidence that regional fat mass accumulations are closely correlated with oxidative stress. Among them, lower-body FM is strongly associated with systemic oxidative stress. In addition, relationships among oxidative stress to inflammatory markers (hsCRP, PAI-1) and adipokines (leptin) were also observe in this healthy female cohort.

To our knowledge, the present study is the first to evaluate the relation between DXA regional adiposity and systemic oxidative stress indicated by urinary 8-epi-$PGF_{2\alpha}$ excretion. We found that indirect anthropometric measures of BMI and WC exhibited strong correlations with oxidative stress. However the value of these simple anthropometric measures in explaining the oxidative stress level was somewhat lower after adjustment for DXA-indices. Thus, although BMI and WC represent an useful markers of oxidative stress, DXA-indices exhibited a better independent power in predicting systemic oxidative stress. The results show that both central and peripheral fat deposits are strongly associated with oxidative stress. And more interestingly, lower-body FM has the strongest relationship with 8-epi-$PGF_{2\alpha}$. Only a few studies evaluated relationship between regional FM and oxidative stress, for example, significant correlation between serum 8-epi-$PGF_{2\alpha}$ level and abdominal visceral fat area (VFA) measured with CT was reported in 31 Japanese men by Urakawa et al. [12]. And Fujita *et al.* [16] reported that in 105 Japanese adults with or without MetS, both abdominal VFA and subcutaneous fat area (SFA) showed significant association with urinary 8-epi-$PGF_{2\alpha}$ excretion, moreover, in multiple regression analysis VFA was the strongest determinant of urinary 8-epi-$PGF_{2\alpha}$ in individuals with MetS. However, these two and other studies only emphasized FM depositing in the abdominal cavity without giving consideration to the effects of total body FM as well as other regional adiposity. Based on CT or magnetic resonance imaging (MRI), it has been estimated that in women the vast majority of FM situated subcutaneously and only 7-8% of the total body FM depots in abdominal cavity [36-38]. Therefore we believe it is more reasonable to take total and regional FM into account when concern with the relation of adiposity to systemic oxidative stress. In the current study, we found total, trunk and lower-body FM showed strong correlations with oxidative stress, even after controlling for BMI and WC. In multiple regression analysis after further taking various confounders into account, lower-body FM and PAI-1 exhibited strong power to predict systemic oxidative stress. Since in women lower-body region is a major compartment for subcutaneous FM accumulation [39, 40], it might be speculated that subcutaneous FM is an important correlate of systemic stress in healthy middle-aged women. The result is somewhat different from Urakawa's [12] and Fujita's [16] findings which suggested abdominal VFA is strongly associated with systemic oxidative stress. This maybe due to we investigate the relationship between adiposity and oxidative stress with a different view of point. General body FM distribution measured with DXA is emphasized in the present study whereas other studies concentrate on the effects of VFA and SAF located in the abdominal cavity estimated with single slice CT scan. Moreover, the subjects we studied are basically lean female adults with mean BMI, WC, FM% as 22.0kg/m^2, 78.9cm and 30.1%, respectively and no one could be classified as having MetS, which are quite different from Urakawa's study (male adults with mean BMI 26.9kg/m^2 and WC 156.9cm in obese group) and Fujita's study (male and female adults with mean BMI 28.7kg/m^2 and WC 96.9cm in MetS group). Unfortunately we are not able to test the association between lower-body FM and oxidative stress after correction for visceral FM because DXA cannot distinguish trunk visceral FM from subcutaneous FM. However, after adjustment for WC, a surrogate index for abdominal visceral FM [41], lower-body FM still associated with oxidative stress in our study.

The underlying mechanism(s) why subcutaneous FM represents a potent link with oxidative stress in healthy female adults is not elucidated yet. Intrinsic different metabolic activity between visceral adipocyte and subcutaneous adipocyte [42], as well as the characteristic of FM distribution of women, may provide explanations. Lipids accumulation is favored in the lower-body region of premenopausal women in comparison with men [43]. This may due to the lipoprotein lipase (LPL) activity, a key factor responsible for the liberation of the lipolytic products to the adipocyte for deposit as TG, is higher in subcutaneous fat cells than visceral adipocyte in women, but not in men [18]. On the other hand, lower-body fat cell exhibits a lower lipolytic response to catecholamine and a higher response to insulin-mediated lipogenesis than visceral adipocyte does, and showing both reduced β1- and β2-adrenoreceptor density and sensitivity and increased α2-adrenoreceptor affinity and number [18, 44, 45]. As

a result, lower-body fat cells in women are resistant to lipolysis and prone to lipogenesis. LPL is demonstrated to be able to enhance both enzymatic and non-enzymatic oxidation of LDL lipids induced by 15-lipoxygenase [46] then elevated LPL activity of lower-body FM may contribute to the activation of lipid peroxidation. Furthermore, animal experiment indicated that during the course of the repeated cycles of fasting-feeding, the changes of lipid peroxidation and lipolysis were antiparallel to each other. That means during the cycles, there was a net increase in lipid peroxidation accompanying with a net decrease in lipolysis [47, 48]. Therefore it is reasonable to assume that the reduced lipolysis in lower-body subcutaneous adipose tissue might result in a heightened lipid peroxidation. Further experiments comparing the lipid peroxidation between visceral and subcutaneous adipose tissue are needed to clarify this issue.

In this study, multiple regression analyses demonstrated that PAI-1 is another important predictor of systemic oxidative stress level. This finding consists with the observation that increased oxidative stress in cultured adipocyte is able to enhance PAI-1 mRNA expression [9] and activates PAI-1 promoter transcription [49]. Elevated PAI-1 levels is proved to be an independent risk for cardiovascular events [50, 51]. Combined with the results from the present study that urinary 8-epi-$PGF_{2\alpha}$ excretion are positively associated with hsCRP and leptin, the findings support that oxidative-stress-induced dysregulation of adipokines and inflammatory markers have already existed even in healthy women without obvious CVD risks.

Potential limitations of our study should be pointed out. Firstly, because of the cross-sectional nature of the present study we are not able to provide a causative conclusion. Second, the subjects we studied were relatively homogenous with lower CVD risks. Although various confounding factors such as sex, age, cigarette smoking and alcohol drinking have been minimized, we should be cautious to apply the conclusion to general population. Thus further extending the study samples to men and other ethnic populations with various CVD risks is needed. Moreover, lower-body FM has been demonstrated to have beneficial effects on glucose [25, 42] and lipid metabolism [17], however our findings suggest that this beneficial metabolic effects of lower-body FM might be mediated by other factors or pathways more than oxidative stress at least in healthy women.

In summary, novel findings of the present study indicate DXA-derived fat mass measures are more potent correlates with systemic oxidative stress than indirect anthropometric indices in healthy middle-aged women. Lower-body FM exhibited strong ability to predict urinary 8-epi-$PGF_{2\alpha}$ excretion, suggesting subcutaneous FM plays an important role in systemic oxidative stress. These results suggest that regional adiposity in the lower-body part should be taken into account as obesity-related phenotypes in evaluating obesity-induced systemic oxidative stress. The interrelationships among urinary 8-epi-$PGF_{2\alpha}$ excretion, PAI-1, hsCRP and leptin, combined with results of other *in vitro* studies, suggest that oxidative-stress-induced dysregulation of adipokines and inflammation might mediate adverse metabolic effects of regional adiposity.

Acknowledgement

This study was supported by Open Research Center Project for Private University: Matching Fund Subsidy for Private Universities, The Ministries of Education, Culture, Sports, Science and Technology, Japan. We are indebted to all the participants for their dedicated and conscientious collaboration.

References

1. Despres JP, Lemieux I (2006) Abdominal obesity and metabolic syndrome. *Nature* 444:881-887.
2. Ford ES (2005) Risks for all-cause mortality, cardiovascular disease, and diabetes associated with the metabolic syndrome: a summary of the evidence. *Diabetes Care* 28:1769-1778.
3. Hotamisligil GS, Shargill NS, Spiegelman BM (1993) Adipose expression of tumor necrosis factor-alpha: direct role in obesity-linked insulin resistance. *Science* 259:87-91.
4. Shimomura I, Funahashi T, Takahashi M, Maeda K, Kotani K, Nakamura T, Yamashita S, Miura M, Fukuda Y, Takemura K, Tokunaga K, Matsuzawa Y (1996) Enhanced expression of PAI-1 in visceral fat: possi-

ble contributor to vascular disease in obesity. *Nat Med* 2:800-803.

5. Emdin M, Pompella A, Paolicchi A (2005) Gammaglutamyltransferase, atherosclerosis, and cardiovascular disease: triggering oxidative stress within the plaque. *Circulation* 112:2078-2080.
6. Itoh S, Umemoto S, Hiromoto M, Toma Y, Tomochika Y, Aoyagi S, Tanaka M, Fujii T, Matsuzaki M (2002) Importance of NAD (P) H oxidase-mediated oxidative stress and contractile type smooth muscle myosin heavy chain SM2 at the early stage of atherosclerosis. *Circulation* 105:2288-2295.
7. Perticone F, Ceravolo R, Candigliota M, Ventura G, Iacopino S, Sinopoli F, Mattioli PL (2001) Obesity and body fat distribution induce endothelial dysfunction by oxidative stress: protective effect of vitamin C. *Diabetes* 50:159-165.
8. Robertson RP (2004) Chronic oxidative stress as a central mechanism for glucose toxicity in pancreatic islet beta cells in diabetes. *J Biol Chem* 279:42351-42354.
9. Furukawa S, Fujita T, Shimabukuro M, Iwaki M, Yamada Y, Nakajima Y, Nakayama O, Makishima M, Matsuda M, Shimomura I (2004) Increased oxidative stress in obesity and its impact on metabolic syndrome. *J Clin Invest* 114:1752-1761.
10. Keaney JF, Jr., Larson MG, Vasan RS, Wilson PW, Lipinska I, Corey D, Massaro JM, Sutherland P, Vita JA, Benjamin EJ (2003) Obesity and systemic oxidative stress: clinical correlates of oxidative stress in the Framingham Study. *Arterioscler Thromb Vasc Biol* 23:434-439.
11. Ferroni P, Guagnano MT, Manigrasso MR, Ciabattoni G, Davi G (2005) Increased plasminogen activator inhibitor-1 levels in android obesity: correlation with oxidative stress. *J Thromb Haemost* 3:1086-1087.
12. Urakawa H, Katsuki A, Sumida Y, Gabazza EC, Murashima S, Morioka K, Maruyama N, Kitagawa N, Tanaka T, Hori Y, Nakatani K, Yano Y, Adachi Y (2003) Oxidative stress is associated with adiposity and insulin resistance in men. *J Clin Endocrinol Metab* 88:4673-4676.
13. Nakanishi S, Yamane K, Kamei N, Nojima H, Okubo M, Kohno N (2005) A protective effect of adiponectin against oxidative stress in Japanese Americans: the association between adiponectin or leptin and urinary isoprostane. *Metabolism* 54:194-199.
14. Shin MJ, Lee JH, Jang Y, Park E, Oh J, Chung JH, Chung N (2006) Insulin resistance, adipokines, and oxidative stress in nondiabetic, hypercholesterolemic patients: leptin as an 8-epi-prostaglandin F2alpha determinant. *Metabolism* 55:918-922.
15. Davi G, Guagnano MT, Ciabattoni G, Basili S, Falco A, Marinopiccoli M, Nutini M, Sensi S, Patrono C (2002) Platelet activation in obese women: role of inflammation and oxidant stress. *JAMA* 288:2008-2014.
16. Fujita K, Nishizawa H, Funahashi T, Shimomura I, Shimabukuro M (2006) Systemic oxidative stress is associated with visceral fat accumulation and the metabolic syndrome. *Circ J* 70:1437-1442.
17. Rebuffe-Scrive M, Lonnroth P, Marin P, Wesslau C, Bjorntorp P, Smith U (1987) Regional adipose tissue metabolism in men and postmenopausal women. *Int J Obes* 11:347-355.
18. Bouchard C, Despres JP, Mauriege P (1993) Genetic and nongenetic determinants of regional fat distribution. *Endocr Rev* 14:72-93.
19. Hamdy O, Porramatikul S, Al-Ozairi E (2006) Metabolic obesity: the paradox between visceral and subcutaneous fat. *Curr Diabetes Rev* 2:367-373.
20. Williams MJ, Hunter GR, Kekes-Szabo T, Snyder S, Treuth MS (1997) Regional fat distribution in women and risk of cardiovascular disease. *Am J Clin Nutr* 65:855-860.
21. Hunter GR, Kekes-Szabo T, Snyder SW, Nicholson C, Nyikos I, Berland L (1997) Fat distribution, physical activity, and cardiovascular risk factors. *Med Sci Sports Exerc* 29:362-369.
22. Van Pelt RE, Evans EM, Schechtman KB, Ehsani AA, Kohrt WM (2002) Contributions of total and regional fat mass to risk for cardiovascular disease in older women. *Am J Physiol Endocrinol Metab* 282:E1023-1028.
23. Roberts LJ, 2nd, Morrow JD (1997) The generation and actions of isoprostanes. *Biochim Biophys Acta* 1345:121-135.
24. Goodpaster BH (2002) Measuring body fat distribution and content in humans. *Curr Opin Clin Nutr Metab Care* 5:481-487.
25. Snijder MB, Dekker JM, Visser M, Bouter LM, Stehouwer CD, Yudkin JS, Heine RJ, Nijpels G, Seidell JC (2004) Trunk fat and leg fat have independent and opposite associations with fasting and postload glucose levels: the Hoorn study. *Diabetes Care* 27:372-377.
26. Mazess RB, Barden HS, Bisek JP, Hanson J (1990) Dual-energy x-ray absorptiometry for total-body and regional bone-mineral and soft-tissue composition. *Am J Clin Nutr* 51:1106-1112.
27. Svendsen OL, Haarbo J, Hassager C, Christiansen C (1993) Accuracy of measurements of body composition by dual-energy x-ray absorptiometry *in vivo*. *Am J Clin Nutr* 57:605-608.
28. Matthews DR, Hosker JP, Rudenski AS, Naylor BA, Treacher DF, Turner RC (1985) Homeostasis model assessment: insulin resistance and beta-cell function from fasting plasma glucose and insulin concentrations in man. *Diabetologia* 28:412-419.
29. Friedewald WT, Levy RI, Fredrickson DS (1972) Estimation of the concentration of low-density lipoprotein cholesterol in plasma, without use of the preparative ultracentrifuge. *Clin Chem* 18:499-502.

30. Hirano T, Ito Y, Saegusa H, Yoshino G (2003) A novel and simple method for quantification of small, dense LDL. *J Lipid Res* 44:2193-2201.
31. (2000) WHO Western Pacific Regional Office, IOTF, IASO, *The Asia-Pacific perspective: redefining obesity and its treatment*, In: Health Communications Australia Sydney.
32. (2001) Executive Summary of The Third Report of The National Cholesterol Education Program (NCEP) Expert Panel on Detection, Evaluation, And Treatment of High Blood Cholesterol In Adults (Adult Treatment Panel III). *JAMA* 285:2486-2497.
33. Alberti KG, Zimmet P, Shaw J (2006) Metabolic syndrome—a new world-wide definition. A Consensus Statement from the International Diabetes Federation. *Diabet Med* 23:469-480.
34. Matsuzawa Y (2005) Metabolic syndrome—definition and diagnostic criteria in Japan. *J Atheroscler Thromb* 12:301.
35. Ceriello A, Motz E (2004) Is oxidative stress the pathogenic mechanism underlying insulin resistance, diabetes, and cardiovascular disease? The common soil hypothesis revisited. *Arterioscler Thromb Vasc Biol* 24:816-823.
36. Sohlstrom A, Wahlund LO, Forsum E (1993) Adipose tissue distribution as assessed by magnetic resonance imaging and total body fat by magnetic resonance imaging, underwater weighing, and body-water dilution in healthy women. *Am J Clin Nutr* 58:830-838.
37. Ludescher B, Najib A, Baar S, Machann J, Thamer C, Schick F, Buchkremer G, Claussen CD, Eschweiler GW (2007) Gender specific correlations of adrenal gland size and body fat distribution: a whole body MRI study. *Horm Metab Res* 39:515-518.
38. Lemieux S, Prud'homme D, Bouchard C, Tremblay A, Despres JP (1993) Sex differences in the relation of visceral adipose tissue accumulation to total body fatness. *Am J Clin Nutr* 58:463-467.
39. Goodpaster BH, Thaete FL, Simoneau JA, Kelley DE (1997) Subcutaneous abdominal fat and thigh muscle composition predict insulin sensitivity independently of visceral fat. *Diabetes* 46:1579-1585.
40. Goodpaster BH, Thaete FL, Kelley DE (2000) Thigh adipose tissue distribution is associated with insulin resistance in obesity and in type 2 diabetes mellitus. *Am J Clin Nutr* 71:885-892.
41. Pouliot MC, Despres JP, Lemieux S, Moorjani S, Bouchard C, Tremblay A, Nadeau A, Lupien PJ (1994) Waist circumference and abdominal sagittal diameter: best simple anthropometric indexes of abdominal visceral adipose tissue accumulation and related cardiovascular risk in men and women. *Am J Cardiol* 73:460-468.
42. Tran TT, Yamamoto Y, Gesta S, Kahn CR (2008) Beneficial effects of subcutaneous fat transplantation on metabolism. *Cell Metab* 7:410-420.
43. Arner P, Lithell H, Wahrenberg H, Bronnegard M (1991) Expression of lipoprotein lipase in different human subcutaneous adipose tissue regions. *J Lipid Res* 32:423-429.
44. Mauriege P, Marette A, Atgie C, Bouchard C, Theriault G, Bukowiecki LK, Marceau P, Biron S, Nadeau A, Despres JP (1995) Regional variation in adipose tissue metabolism of severely obese premenopausal women. *J Lipid Res* 36:672-684.
45. Reynisdottir S, Wahrenberg H, Carlstrom K, Rossner S, Arner P (1994) Catecholamine resistance in fat cells of women with upper-body obesity due to decreased expression of beta 2-adrenoceptors. *Diabetologia* 37:428-435.
46. Neuzil J, Upston JM, Witting PK, Scott KF, Stocker R (1998) Secretory phospholipase A2 and lipoprotein lipase enhance 15-lipoxygenase-induced enzymic and nonenzymic lipid peroxidation in low-density lipoproteins. *Biochemistry* 37:9203-9210.
47. Rejholcova M, Wilhelm J (1989) Lipid peroxidation and lipolysis during fasting. *Acta Univ Carol [Med]* (Praha) 35:43-61.
48. Rejholcova M, Wilhelm J, Svoboda P (1988) Lipid peroxidation inhibits norepinephrine- stimulated lipolysis in rat adipocytes. Reduction of beta-adreno-ceptor number. *Biochem Biophys Res Commun* 150:802-810.
49. Vulin AI, Stanley FM (2004) Oxidative stress activates the plasminogen activator inhibitor type 1 (PAI-1) promoter through an AP-1 response element and cooperates with insulin for additive effects on PAI-1 transcription. *J Biol Chem* 279:25172-25178.
50. Landin K, Tengborn L, Smith U (1990) Elevated fibrinogen and plasminogen activator inhibitor (PAI-1) in hypertension are related to metabolic risk factors for cardiovascular disease. *J Intern Med* 227:273-278.
51. Juhan-Vague I, Alessi MC (1997) PAI-1, obesity, insulin resistance and risk of cardiovascular events. *Thromb Haemost* 78:656-660.

Laboratory Investigation (2009) 89, 1340–1347

Timp-3 deficiency impairs cognitive function in mice

Yoshichika Baba[1], Osamu Yasuda[1], Yukihiro Takemura[1], Yasuyuki Ishikawa[2], Mitsuru Ohishi[1], Jun Iwanami[3], Masaki Mogi[3], Nobutaka Doe[4], Masatsugu Horiuchi[3], Nobuyo Maeda[5], Keisuke Fukuo[6] and Hiromi Rakugi[1]

Extracellular matrix (ECM) degradation is performed primarily by matrix metalloproteinases (MMPs). MMPs have recently been shown to regulate synaptic activity in the hippocampus and to affect memory and learning. The tissue inhibitor of metalloproteinase (Timp) is an endogenous factor that controls MMP activity by binding to the catalytic site of MMPs. At present, four Timp isotypes have been reported (Timp-1 through Timp-4) with 35–50% amino-acid sequence homology. Timp-3 is a unique member of Timp proteins in that it is bound to the ECM. In this study, we used the passive avoidance test, active avoidance test, and water maze test to examine the cognitive function in Timp-3 knockout (KO) mice. Habituation was evaluated using the open-field test. The water maze test showed that Timp-3 KO mice exhibit deterioration in cognitive function compared with wild-type (WT) mice. The open-field test showed decreased habituation of Timp-3 KO mice. Immunostaining of brain slices revealed the expression of Timp-3 in the hippocampus. *In situ* zymography of the hippocampus showed increased gelatinolytic activity in Timp-3 KO mice compared with WT mice. These results present the first evidence of Timp-3 involvement in cognitive function and hippocampal MMP activity in mice. Moreover, our findings suggest a novel therapeutic target to be explored for improvement of cognitive function in humans.

Laboratory Investigation (2009) **89,** 1340–1347; doi:10.1038/labinvest.2009.101; published online 5 October 2009

KEYWORDS: cognitive function; extracellular matrix; hippocampus; matrix metalloproteinase; Timp-3

Extracellular matrix (ECM) molecules have important roles in the structural changes of brain synapses involved in neural plasticity, learning, and memory.[1] ECM interacts with cells through cell surface receptors, such as integrin, cadherin, and neural adhesion molecules,[2] and these interactions affect cell proliferation, growth, migration, synaptic stabilization, and apoptosis. Thus, the ECM develops a wide range of signals within the brain tissue.[3]

Matrix metalloproteinases (MMPs) comprise a family of protein-digesting enzymes that have an important role in structural maintenance and conversion of the ECM.[4] MMPs target many substrates, including proteases, growth factors, cytokines, cell surface receptors, and cell adhesion molecules.[5] Excess activation of MMPs occurs under several pathophysiological conditions, such as rheumatoid arthritis and rupture of atherosclerotic plaques.[6–8] Thus, MMP activity is tightly controlled at the level of transcription, activation of the precursor zymogens, and inhibition by the tissue inhibitors of metalloproteinase (Timp).[9]

At present, four members of the Timp family (Timp-1 to Timp-4), possessing 35–50% amino-acid sequence homology, have been identified. All Timp isotypes contain 12 cysteines that form 6 disulfide bonds. To inhibit MMP activity, Timp proteins form a 1:1 complex with a zinc-binding site in the catalytic region of MMP.[10]

Each Timp protein has unique characteristics. Timp-1, Timp-2, and Timp-4 are present in soluble form.[11–13] Timp-3, which is tightly bound to the ECM, is involved in cell proliferation, apoptosis, and angiogenesis.[11–13] Timp-1 binds to proMMP-9, Timp-2 binds to proMMP-2, and Timp-3 binds to both proMMP-2 and proMMP-9.[13,14]

In the central nervous system, the MMP/Timp system is responsive to changes in neural activity.[15] Deregulation of MMP activity is involved in various neurological diseases,

[1]Department of Geriatric Medicine, Osaka University Graduate School of Medicine, Suita, Osaka, Japan; [2]Division of Structural Cell Biology, Nara Institute of Science and Technology, Takayama-cho, Ikoma, Nara, Japan; [3]Department of Molecular Cardiovascular Biology and Pharmacology, Ehime University, Graduate School of Medicine, Shitsukawa, Tohon, Ehime, Japan; [4]Section of Behavioral Science, Kouiken Co. Ltd., Akashi, Hyogo, Japan; [5]Department of Pathology and Laboratory Medicine, School of Medicine, The University of North Carolina at Chapel Hill, Chapel Hill, NC, USA and [6]Department of Food Sciences and Nutrition, School of Human Environmental Sciences, Mukogawa Woman's University, Nishinomiya, Hyogo, Japan

Correspondence: Dr O Yasuda, MD, PhD, Department of Geriatric Medicine, Osaka University Graduate School of Medicine, 2-2 Yamadaoka, Suita, Osaka 565-0871, Japan.

E-mail: yasuda@geriat.med.osaka-u.ac.jp

Received 16 February 2009; revised 27 July 2009; accepted 20 August 2009

including multiple sclerosis, infection with human immunodeficiency virus, and spinal cord injury.[16–18] Moreover, MMPs are implicated in the invasion of malignant glioma cells into the brain parenchyma.[19]

In Alzheimer's disease, MMP inhibits angiogenesis and accumulation of amyloid-β.[16,20,21] Recently, MMPs have been reported to control synaptic activity in the hippocampus and to affect learning and memory.[22] Other studies have clarified the contributions of Timp-1 and Timp-2 in learning and memory. Mice deficient for Timp-1 or Timp-2 exhibit defective memory function.[23–25] Conversely, mice overexpressing Timp-1 showed a slight, but significant, improvement in learning and memory.[24] However, there is no published evidence for a role of Timp-3 in the regulation of cognitive function.

This study investigated the effects of Timp-3 on learning and memory. We conducted various behavioral tests with wild-type (WT) and Timp-3 knockout (KO) mice, and further examined the expression of Timp-3 and compared gelatinolytic activity in WT and KO brain tissues.

MATERIALS AND METHODS

Timp-3 KO Mice

Timp-3 KO mice were produced using the gene-targeting technique described by Kawamoto *et al*.[26] Briefly, mice carrying the mutant allele were backcrossed with C57BL/6 mice to generate KO mice in a C57BL/6 background. Genotyping of mice was performed by PCR using tail DNA.[26]

Experimental Conditions for Behavioral Tests

All behavioral tests were conducted in the laboratory at 22 °C and 55% (50–60%) humidity. Illumination for the experimental device was set at 250 lx. The ventilation fan provided a masking noise of 40 dB, which was deemed appropriate for behavioral tests.

Mice were maintained in individual acrylic cages and naturalized to the environment during the 3 days before testing. They were given access to dry, solid feed (Labo MR Stock from Nihon Nosan, Yokohama, Japan) *ad libitum*. The room was maintained on a 12-h light and dark cycle, with the light cycle starting at 0800 hours and ending at 2000 hours. All tests were started after 1000 hours and conducted during the light period.

The passive avoidance test and water maze test with an invisible platform were conducted with 12 male WT mice and 12 KO mice. The open-field habituation test, active avoidance test, and water maze test with a visible platform were conducted using a different set of 12 male WT mice and 12 KO mice.

The experimental protocols were approved by the Osaka University Medical School Animal Care and Use Committee, and performed according to the Osaka University Medical School Guidelines for the Care and Use of Laboratory Animals.

Passive Avoidance Test

An avoidance-learning box was constructed, with a lighted chamber ($15 \times 15 \times 20\,cm^3$) and dark chamber ($15 \times 15 \times 20\,cm^3$) connected to each other. A guillotine door separated the two compartments. A mouse was placed in the lighted chamber, and the guillotine door was opened. When the mouse spontaneously moved into the dark chamber, the guillotine door was closed. Within 10 s, a 3-s, 160-V AC electrical shock was delivered through the grid floor. The latency period for the mouse to enter the dark chamber was recorded. After this single learning trial, the mouse was immediately removed from the device.

After 24 h, the same mouse was put in the lighted chamber for the single retention test. The latency period (≤ 300 s) for the mouse to enter the dark chamber was recorded. No electric shock was given during the retention test.

Active Avoidance Test

An avoidance-learning box with two connecting compartments (each $15 \times 15 \times 20\,cm^3$) was constructed. The mouse was able to move freely between the two compartments. To detect movement, two infrared ray beams were attached on both walls on the sides of each compartment, 2 cm above the floor and 5 cm from the gate. The avoidance-learning box, which was placed in a ventilated, sound-attenuating chamber to maintain a background noise level of 64 dB throughout the session, was indirectly illuminated by white bulbs fixed to the ceiling of the chamber. A 1500-Hz pure tone with 85 dB of sound pressure was used as a conditioned stimulus (CS), and a 140-V AC electrical shock delivered from the grid floor was used as an unconditioned stimulus (US).

A mouse was placed in one compartment and allowed to move between the two compartments throughout the training session. The US, which was delivered from the grid floor 5 s after the CS was delivered, overlapped for a maximum of 15 s. When the mouse moved to the connecting compartment within 5 s from the time of the CS, the US was not delivered, and the movement of the mouse was counted as avoidance behavior. When the mouse failed to move to the connecting compartment, the US was delivered. Both the CS and US were terminated immediately when the mouse moved to the connecting compartment after the onset of the US. The number of migration reactions in inter-trial intervals (25 s on average) was measured as an indicator of spontaneous activity. This active avoidance test was performed for 3 consecutive days, with one 50-trial session per day.

Water Maze Test

The water maze test was conducted using a round pool (inside diameter = 95 cm; depth = 35 cm) filled with water, made opaque by the addition of titanium oxide to a depth of 22 cm. The temperature of the water was maintained at 22 ± 1 °C using a thermostatic heater. The pool was set on a pedestal (30 cm in height), and was enclosed (area = $130 \times 130\,cm^2$) by four white walls (120 cm in

height). As extra-maze cues, letter-sized posters, a CCD camera, and a black doll (20 cm in height) were attached to the walls.

In the invisible platform test, a clear, round platform (diameter = 10 cm) was submerged 0.5 cm below the surface of the water. Training trials were conducted for 5 consecutive days, with 5 trial sessions per day. In the three quadrants away from the platform, a mouse placed near the wall was released into the pool. The releasing quadrants varied with pseudo-random sequences for each mouse. The escape latency period (measured for a maximum of 60 s) was defined as the time it took for a mouse to reach the platform. The training trial terminated when the mouse reached the platform and remained on it for 10 s. In cases in which the mouse did not find the platform within 60 s, the mouse was guided to the platform by the experimenter and was kept on the platform for 10 s. On the day after 5 consecutive days of access training, the platform was removed, and a 1-min probe test was performed. The 1-min probe test measured latency time in the quadrant in which the platform was previously placed.

The visible platform test was conducted independently using a different group of 12 WT and 12 KO mice (ie, different groups of mice from those used in the invisible platform test). Methodology for the visible platform test was similar, except (1) the platform was not submerged, but rather was placed 0.5 cm above the surface of the water, and (2) as a cue, a stick with a black cube on top was placed on the platform.

Open-Field Habituation Test

The apparatus for the open-field habituation test was manufactured by Taiyo Electric. (Tokyo, Japan). WT and KO mice were placed in an acrylic box ($30 \times 30 \times 30\,cm^3$) stored within a ventilated, soundproof chamber. An incandescent bulb, which was fixed to the ceiling of the chamber, provided lighting of ~110 lx in the chamber. A fan attached to the wall of the chamber produced a masking noise of 45 dB. Habituation of the mice to the environment was measured as a function of locomotion and rearing behavior. The number of episodes of locomotion and rearing behavior, which were recorded with infrared ray beams placed on the lateral side of the box, was scored. The open-field habituation test was conducted for 3 days, with one 10-min session per day.

Reverse Transcription-PCR

RNA was isolated from mouse hippocampus using the ISOGEN (Nippon Gene, Tokyo, Japan) kit, according to the manufacturer's instructions. *Timp-3* gene expression was detected by reverse transcribing the isolated RNA and amplifying the product with PCR (RT-PCR). The PCR amplification was performed with the following primers: Timp-3: Timp-3F, 5′-CACGGAAGCCTCTGAAAGTC-3′, and Timp-3R, 5′-CCCAAAATTGGAGAGCATGT-3′. GAPDH: GAPDH-F, 5′-AAATGGTGAAGGTCGGTGTG-3′, and GAPDH-R, 5′-GCAGAAGGGGCGGAGATGAT-3′.

Immunostaining

WT and Timp-3 KO mice were killed, and their brains were collected, fixed with formaldehyde, embedded in paraffin, and cut into 10-μm-thick sections with a microtome. To remove endogenous peroxidase, the sections were treated with 0.3% hydrogen peroxide in methanol at room temperature. The sections were washed with 0.05 M phosphate buffer (pH 7.6) thrice for 3 min. The sections were then treated with phosphate buffer containing 0.5% bovine serum albumin and 0.1% sodium azide for 10 min at room temperature. This was performed to absorb nonspecific proteins. Subsequently, the sections were allowed to react with the anti-Timp-3 rabbit polyclonal antibody (ProteinTech, Chicago, IL, USA) (500 × dilution) overnight at 4 °C. Next, the sections were washed thrice for 3 min with 0.05 M phosphate buffer (pH 7.6), and then allowed to react for 30 min with the secondary antibody conjugated with peroxidase. Thereafter, the sections were again washed with 0.05 M phosphate buffer. After a 5-min chromogenic reaction with 3,3′-Diaminobenzidine HCl, the sections were counterstained with Mayer's hematoxylin for 5 min. The sections were then dehydrated and encapsulated for observation under an optical microscope.

In Situ Zymography

Gelatinolytic activity in mouse brain sections was determined by *in situ* zymography with DQ-gelatin-FITC (Molecular Probes, Eugene, OR, USA) as described previously.[27,28] Briefly, unfixed whole mouse brain was embedded in OCT compound. Sections (of 10-μm thickness) were cut and air dried for 1 h, re-hydrated in PBS, and incubated at 37 °C in DQ-gelatin-FITC solution (100 μg/ml in PBS) for 1 h. Sections were then washed thrice in PBS, fixed in 4% paraformaldehyde, and examined under a fluorescent microscope to detect green fluorescence due to gelatinolytic activity.

Statistical Analysis

Results are expressed as mean ± s.e. Comparison among groups was performed by one-way ANOVA; Student's *t*-test was used when appropriate. A value of $P<0.05$ was considered significant.

RESULTS

Passive Avoidance Test

WT and KO mice first underwent preconditioning. When a mouse moved from the lighted chamber into the dark chamber, it received an electric shock. Twenty-four hours after preconditioning, one retention trial was performed. In the retention trial, the latency time in the lighted chamber was measured and compared between the two mice groups. As a result of receiving an electric shock in the dark chamber, the mean latency time in the retention trial was prolonged in

both WT and KO mice, indicating that both types of mice acquired avoidance memory. Moreover, no significant difference was observed in latency times for WT and KO mice, either before (54.4 ± 19.5 s for WT, 27.7 ± 7.5 s for KO; $P = 0.20$) or after (300 ± 0.0 s for WT, 276 ± 18.7 s for KO; $P = 0.23$) conditioning. These results show that there were no memory deficits in KO mice compared with WT mice.

Active Avoidance Test

WT and KO mice were placed in the avoidance-learning box with two compartments connected. A beep was presented, and 5 s later, an electronic shock was given through the grid floor. When this process was repeated, the mice learned to escape the shock by migrating into the adjoining compartments at the sound of the beep. A migration reaction within 5 s from the beep was defined as the 'avoidance' reaction. The number of avoidance reactions was counted over 3 days, with 50 trials per day. Moreover, the number of migrations between trial intervals in the absence of stimuli was counted to compare general activity levels.

We found no differences in activity levels between WT and KO mice over the 3 days of testing ($F(1,22) = 1.88$, $P = 0.183$). Successful avoidance increased in both WT and KO mice as a function of training days, indicating that both types of mice acquired avoidance memory. Furthermore, there was no difference between the number of avoidance reactions in WT and KO mice during the 3 days of testing ($F(1,22) = 0.46$, $P = 0.505$). These results indicate that no memory deficits were detected in KO mice.

Water Maze Test with Invisible Platform

The water maze test with the invisible platform was conducted to evaluate spatial memory in WT and KO mice. Each mouse underwent 5 access tests daily for 5 consecutive days. Escape latency period was defined as the time (measured for a maximum of 60 s) it took for each mouse to reach the platform submerged in the pool of opaque water.

On the first day, no significant difference was observed between WT and KO mice. However, on the second day, memory acquisition in KO mice was significantly reduced compared with WT mice. Although a significant difference in memory acquisition was also observed on the third and fourth days, the difference gradually decreased (Figure 1a), and the difference in memory acquisition was no longer significant on day 5.

To measure the time spent in the quadrant in which the platform had been previously placed, a 1-min probe test was conducted the day after (ie, on day 6) completion of the access tests. The time spent in the target quadrant was longer than that achieved merely by chance, indicating that both types of mice acquired memory of the previous location of the platform. Moreover, no significant difference was observed in the time that WT or KO mice spent in the target quadrant (19.6 ± 1.71 s for WT; 20.9 ± 1.27 s for KO; $P = 0.561$).

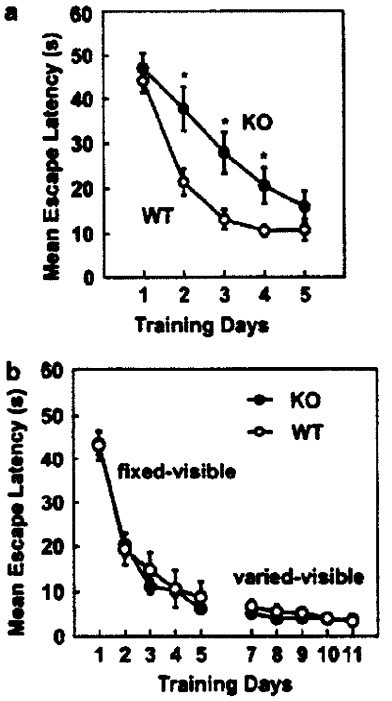

Figure 1 Water maze tests. (**a**) Invisible platform test of wild-type (WT; $n = 12$) and Timp-3 knockout (KO; $n = 12$) mice. A clear, round platform was submerged 0.5 cm beneath the surface of milk-colored water in a pool. Escape latency period is the time (measured for a maximum of 60 s) it took for each mouse entering the pool to reach the submerged, invisible platform. Training trials were performed for 5 consecutive days, with 5 trial sessions per day. Data are expressed as mean ± s.e. $^*P < 0.05$. (**b**) Visible platform test of WT ($n = 12$) and Timp-3 KO ($n = 12$) mice. The platform was placed 0.5 cm above the surface of water in a pool. As a visual cue, a stick with a black cube on top was placed on the platform. The location of the platform was fixed from day 1 through day 5, and varied from day 7 through day 11. Escape latency period (measured for a maximum of 60 s) is the time it took for each mouse, after entering the pool, to reach the visible platform. Five trial sessions were performed per day. Data are expressed as mean ± s.e.

Taken together, these results indicate that although KO mice eventually learned the location of the platform, their speed in acquiring memory was significantly slower than that of WT mice.

Water Maze Test with Visible Platform

In humans, a Timp-3 mutation causes Sorsby's fundus dystrophy (SFD), a disease characterized by the loss of central vision during the fourth or fifth decade of life. It is likely that the KO mice used in this study were able to recognize visual cues, given that they eventually learned the location of the platform. This conclusion is supported by a previous study showing that learning in water maze tests relies on the use of visual cues.[29] To further investigate whether KO mice were able to use visual cues during a water maze test, a visible platform test was conducted.

The mean escape latency period gradually decreased from day 1 to day 5 in both WT and KO mice, indicating that both types of mice acquired memory of the location of the platform (Figure 1b). Mean escape latency times for WT and KO mice were similar during the 5 days of testing. This finding indicates that both types of mice approached the platform aided by the visible cue, rather than by spatial memory. Moreover, the results suggest that the swimming ability of KO mice was not compromised. Moreover, latency times of WT and KO mice were not different, even when the location of the visible platform was varied (on days 7 through 11). The fact that latency time at day 7, the first day in the varied visible platform test, was not longer than that at day 5, the last day in the fixed visible platform test, also indicates that both types of mice approached the platform aided by the visual cue rather than by spatial memory.

Probe tests conducted on day 6 (13.0 ± 1.40 s for WT; 15.4 ± 0.97 s for KO; $P = 0.162$) and day 12 (12.5 ± 1.18 s for WT; 12.9 ± 0.98 s for KO; $P = 0.821$) also showed no difference in latency times between WT and KO mice. Furthermore, latency times observed for both types of mice were not longer than the latency times expected if achieved merely by chance. These results also indicate that movement of mice in the visible platform test was dependent on the use of visual cues, rather than on memory of the location of the platform.

Taken together, our findings suggest that KO mice were able to recognize visual cues in the water maze test. An alternative interpretation is that visual failure in KO mice was minimal and did not substantially compromise the recognition of visual cues.

Open-Field Habituation Test

To evaluate the motion and mobility of the mice, the numbers of locomotion and rearing were scored for 10 min per day for 3 days with sensors placed on the lateral side of the chamber. There was no significant difference between WT and KO mice in the numbers of locomotion (107.8 ± 5.76 in WT, 116.9 ± 10.76 in KO; $P = 0.490$) and rearing (99.2 ± 6.95 in WT, 91.6 ± 9.19 in KO; $P = 0.535$) on day 1; however, significant differences were observed on day 3 (Figure 2a and b). Both locomotion and rearing decreased over time in WT mice, but did not substantially change over time in KO mice. This indicated that WT, but not KO, mice became accustomed to the environment.

Timp-3 Expression in the Brain

RT-PCR showed the expression of Timp-3 in the hippocampus of WT mice (Figure 3a). In contrast, no Timp-3 was

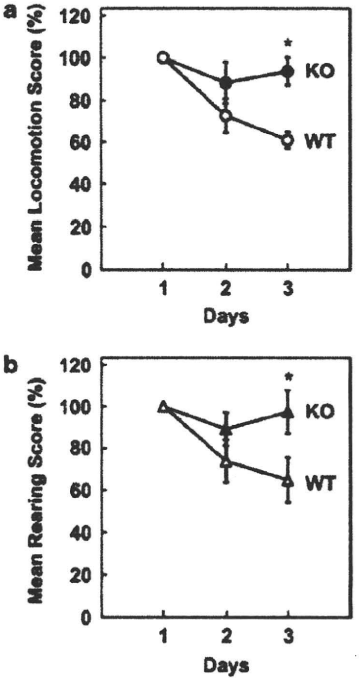

Figure 2 Open-field habituation test. (**a**) The graph shows the change in locomotion score for WT ($n = 12$) and Timp-3 KO ($n = 12$) mice over time (days). The locomotion score, which represents the number of migrations of each mouse in a period of 10 min, is expressed as a percentage. Data are expressed as mean ± s.e. $^*P < 0.05$. (**b**) The graph shows changes in rearing score in WT ($n = 12$) and Timp-3 KO ($n = 12$) mice over time (days). The rearing score, which represents the number of times that each mouse rose (ie, exhibited rearing behavior) in a period of 10 min, is expressed as a percentage. Data are expressed as mean ± s.e. $^*P < 0.05$.

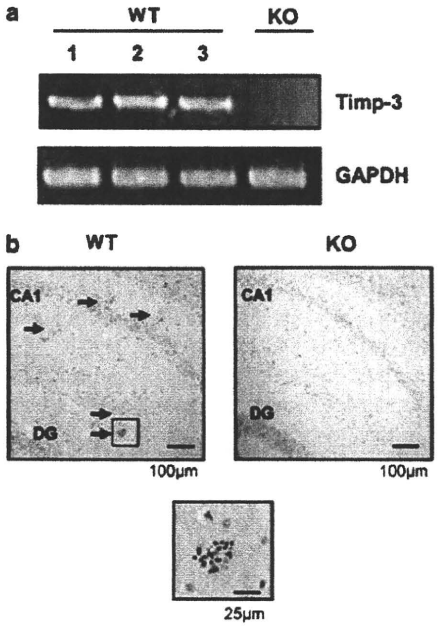

Figure 3 Expression of Timp-3 in the hippocampus. (**a**) RT-PCR of the *Timp-3* gene. RT-PCR was performed with RNA isolated from the hippocampus of wild-type (WT) and three different Timp-3 knockout (KO) mice. Amplification of the glyceraldehyde-3-phosphate dehydrogenase gene (GAPDH) served as a control. (**b**) Immunostaining of Timp-3. A Timp-3 antibody was hybridized to mouse brain sections and visualized with 3-3′-diaminobenzidine and a hematoxylin counterstain. Timp-3 expression is indicated in the hippocampus with arrows. The boxed region shown below is magnified ×4 to illustrate Timp-3 staining. DG, dentate gyrus.

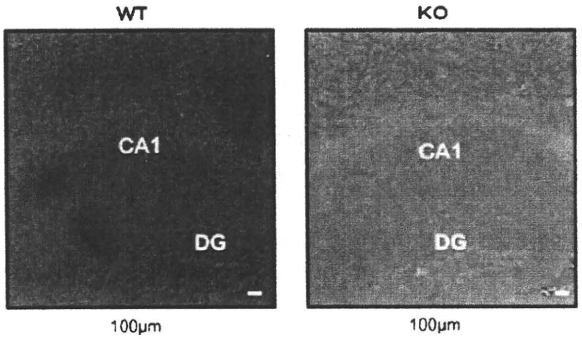

Figure 4 *In Situ* zymography. *In situ* zymography shows the gelatinolytic activity (green fluorescence) of enzymes in the brains of wild-type (WT) and Timp-3 knockout (KO) mice. Representative photographs are shown. DG, dentate gyrus.

detected in the hippocampus of KO mice. Timp-3 expression was confirmed by immunostaining brain slices. Timp-3 was expressed in the choroid plexus (not shown) and in the hippocampus (Figure 3b). This was consistent with the results from the water maze test, because the hippocampus is considered to be directly involved in memory process.

In Situ Zymography

In situ zymography showed that gelatinolytic activity was enhanced in the hippocampus of KO mice compared with that of WT mice. This result was reproducible in four independent experiments. Data from a representative experiment are shown in Figure 4. This result indicated that gelatinolytic enzyme activity was more active in the KO than in WT mice brains.

DISCUSSION

The ECM in a normal, healthy tissue is maintained by a balance of synthesis and degradation, and has a significant role in maintaining tissue homeostasis. In the central nervous system, the balance between Timp and MMP is believed to be involved in synaptic plasticity, particularly in the mechanisms underlying memory. Previous reports have shown that ECM molecules activated signal transduction pathways through diverse cell surface receptors.[1] For example, integrins, the primary laminin receptors, are expressed in the adult hippocampus[30] and are involved in the stabilization of LTP.[31] In this paper, we have shown that Timp-3 KO mice showed increased MMP activity in the hippocampus and impaired cognitive function compared with WT mice. Similarly, Timp-1-deficient mice also showed learning and memory disturbances.[23,24] This result could also be explained by the fact that Timp-1 is expressed in the hippocampus, and synaptic plasticity is influenced by an increase in MMP activity. Timp-2 is also suggested to be involved in synaptic plasticity underlying learning and memory.[25]

We conducted behavioral tests and brain tissue analyses in Timp-3 KO mice to clarify the involvement of Timp-3 in cognitive function. Three behavioral tests were used to evaluate memory function, and an open-field test was used to evaluate habituation. We detected a decline in memory function in KO mice in the water maze test with the invisible platform, but not in passive or active avoidance tests.

Immunostaining showed the presence of Timp-3 in the hippocampus, which is considered to be the main brain region involved in memory. Moreover, *in situ* zymography showed that the hippocampi of Timp-3 KO mice had more gelatinolytic activity than did WT mice, indicating that MMP activity was deregulated in Timp-3 KO mice. Whether hippocampal deregulation of enzymatic activity in Timp-3 KO mice is directly or indirectly involved in delayed acquisition of memory in the water maze test remains to be elucidated. Moreover, it is not known whether other regions of the brain contribute to the abnormality observed in Timp-3 KO mice. Consistent with a previous report, Timp-3 expression was also detected in the choroid plexus.[32]

During central nervous system development, Timp-3 is expressed in the embryonic ventricular zone and postnatal subventricular zone, where neurogenesis occurs.[33] In addition, Timp-3 is expressed in the rostral migratory stream; a sub-population of cells in the subventricular zone migrates along the rostral migratory stream to the olfactory bulb, where cells differentiate into neurons. It is possible that lack of Timp-3 expression during brain development might have long-term effects on cognition, given that impaired cognitive function was observed in adult Timp-3 KO mice in this study.

In the water maze test using a visible platform, Timp-3 KO mice were able to use visual cues to reach the platform. However, in humans mutations in the Timp-3 gene result in SFD, a disease characterized by the loss of central vision during the fourth or fifth decade of life. A possible explanation for the discrepancy is that the Timp-3 KO mice we used were relatively young (3 months old). Alternatively, the difference in the nature of genetic alterations in SFD patients *versus* Timp-3 KO mice is another possibility. Most mutations observed in the *Timp-3* gene in SFD patients involve either the introduction of a new cysteine residue in the C-terminal domain or the presence of an odd number of cysteine residues because of the introduction of a stop codon.[34] Some of these SFD mutations may result in production of higher molecular-weight protein complexes, possibly dimers.[35] Dimerized Timp-3 protein has an active role in the SFD disease process by accumulating in the eyes.[35] In a study of eye tissues obtained from SFD patients, the thickened Bruch's membrane was strongly Timp-3 positive, except for sites where the retinal pigment epithelial cells, which normally produce Timp-3, had degenerated.[36] In contrast, Timp-3 KO mice do not express Timp-3 transcripts, do not synthesize Timp-3 protein, and do not accumulate Timp-3 protein in the eye tissue. On the basis of these observations,

we do not find it too surprising that Timp-3 KO mice were able to recognize visual cues.

The results of the open-field test indicated that habituation was functional in WT mice, but seemed to be lacking in KO mice. This may be because KO mice were unable to remember the environment over time, and thus could not habituate during the test period. It is also possible that the KO mice had a neurological disorder that will impair both memory and habituation.

Timp-3 has been shown to have various functions in previous reports that described other phenotypes of Timp-3 KO mice. For example, at the age of 21 months, Timp-3 KO mice exhibited left ventricular enlargement similar to that observed in dilated cardiomyopathy, cardiac muscle cell hypertrophy, and contractile dysfunction.[37] Others reported that Timp-3 KO mice exhibited a spontaneous air space enlargement in the lung, and enhanced collagen degradation in the peribronchiolar space.[38] In addition, Timp-3 was reportedly involved in apoptosis, cell proliferation, inhibition of cell proliferation, and angiogenesis. However, this study showed for the first time that Timp-3 deficiency impaired cognitive dysfunction, potentially through the deregulation of ECM homeostasis within the brain.

ACKNOWLEDGEMENTS

We thank Ms Taeko Kaimoto for excellent secretarial and technical assistance. This study was supported by a grant in aid for Scientific Research from the Ministry of Education, Science, Sports, and Culture, Japan, and by a grant from the Japan Foundation for Applied Enzymology.

DISCLOSURE/CONFLICT OF INTEREST

The authors declare no conflict of interest.

1. Dityatev A, Schachner M. Extracellular matrix molecules and synaptic plasticity. Nat Rev Neurosci 2003;4:456–468.
2. Dityatev A, Schachner M. The extracellular matrix and synapses. Cell Tissue Res 2006;326:647–654.
3. Wright JW, Harding JW. The brain angiotensin system and extracellular matrix molecules in neural plasticity, learning, and memory. Prog Neurobiol 2004;72:263–293.
4. Nagase H, Woessner Jr JF. Matrix metalloproteinases. J Biol Chem 1999;274:21491–21494.
5. Milward EA, Fitzsimmons C, Szklarczyk A, *et al.* The matrix metalloproteinases and CNS plasticity: an overview. J Neuroimmunol 2007;187:9–19.
6. Firestein GS. Evolving concepts of rheumatoid arthritis. Nature 2003;423:356–361.
7. Tsunemi K, Takai S, Nishimoto M, *et al.* Possible roles of angiotensin II-forming enzymes, angiotensin converting enzyme and chymase-like enzyme, in the human aneurysmal aorta. Hypertens Res 2002;25: 817–822.
8. Iwashima Y, Horio T, Kuroda S, *et al.* Influence of plasma aldosterone on left ventricular geometry and diastolic function in treated essential hypertension. Hypertens Res 2002;25:49–56.
9. Higuchi M, Yasuda O, Kawamoto H, *et al.* Tissue inhibitor of metalloproteinase-3 deficiency inhibits blood pressure elevation and myocardial microvascular remodeling induced by chronic administration of Nomega-nitro-L-arginine methyl ester in mice. Hypertens Res 2007;30:563–571.
10. Brew K, Dinakarpandian D, Nagase H. Tissue inhibitors of metalloproteinases: evolution, structure and function. Biochim Biophys Acta 2000;1477:267–283.
11. Leco KJ, Khokha R, Pavloff N, *et al.* Tissue inhibitor of metalloproteinases-3 (TIMP-3) is an extracellular matrix-associated protein with a distinctive pattern of expression in mouse cells and tissues. J Biol Chem 1994;269:9352–9360.
12. Fedak PW, Verma S, Weisel RD, *et al.* Cardiac remodeling and failure: from molecules to man (Part II). Cardiovasc Pathol 2005;14:49–60.
13. Lambert E, Dasse E, Haye B, *et al.* TIMPs as multifacial proteins. Crit Rev Oncol Hematol 2004;49:187–198.
14. Nagase H, Visse R, Murphy G. Structure and function of matrix metalloproteinases and TIMPs. Cardiovasc Res 2006;69:562–573.
15. Dzwonek J, Rylski M, Kaczmarek L. Matrix metalloproteinases and their endogenous inhibitors in neuronal physiology of the adult brain. FEBS Lett 2004;567:129–135.
16. Agrawal SM, Lau L, Yong VW. MMPs in the central nervous system: where the good guys go bad. Semin Cell Dev Biol 2008; 19:42–51.
17. Yong VW, Power C, Forsyth P, *et al.* Metalloproteinases in biology and pathology of the nervous system. Nat Rev Neurosci 2001;2: 502–511.
18. Yong VW, Krekoski CA, Forsyth PA, *et al.* Matrix metalloproteinases and diseases of the CNS. Trends Neurosci 1998;21:75–80.
19. Park JB, Kwak HJ, Lee SH. Role of hyaluronan in glioma invasion. Cell Adh Migr 2008;2:202–207.
20. Ulrich R, Baumgartner W, Gerhauser I, *et al.* MMP-12, MMP-3, and TIMP-1 are markedly upregulated in chronic demyelinating theiler murine encephalomyelitis. J Neuropathol Exp Neurol 2006;65: 783–793.
21. Yong VW. Metalloproteinases: mediators of pathology and regeneration in the CNS. Nat Rev Neurosci 2005;6:931–944.
22. Ethell IM, Ethell DW. Matrix metalloproteinases in brain development and remodeling: synaptic functions and targets. J Neurosci Res 2007;85:2813–2823.
23. Jourquin J, Tremblay E, Bernard A, *et al.* Tissue inhibitor of metalloproteinases-1 (TIMP-1) modulates neuronal death, axonal plasticity, and learning and memory. Eur J Neurosci 2005;22: 2569–2578.
24. Chaillan FA, Rivera S, Marchetti E, *et al.* Involvement of tissue inhibition of metalloproteinases-1 in learning and memory in mice. Behav Brain Res 2006;173:191–198.
25. Jaworski DM, Boone J, Caterina J, *et al.* Prepulse inhibition and fear-potentiated startle are altered in tissue inhibitor of metalloproteinase-2 (TIMP-2) knockout mice. Brain Res 2005;1051:81–89.
26. Kawamoto H, Yasuda O, Suzuki T, *et al.* Tissue inhibitor of metalloproteinase-3 plays important roles in the kidney following unilateral ureteral obstruction. Hypertens Res 2006;29:285–294.
27. Amantea D, Corasaniti MT, Mercuri NB, *et al.* Brain regional and cellular localization of gelatinase activity in rat that have undergone transient middle cerebral artery occlusion. Neuroscience 2008; 152:8–17.
28. Mook OR, Van Overbeek C, Ackema EG, *et al.* In situ localization of gelatinolytic activity in the extracellular matrix of metastases of colon cancer in rat liver using quenched fluorogenic DQ-gelatin. J Histochem Cytochem 2003;51:821–829.
29. Upchurch M, Wehner JM. Differences between inbred strains of mice in Morris water maze performance. Behav Genet 1988;18: 55–68.
30. Schuster T, Krug M, Stalder M, *et al.* Immunoelectron microscopic localization of the neural recognition molecules L1, NCAM, and its isoform NCAM180, the NCAM-associated polysialic acid, beta1 integrin and the extracellular matrix molecule tenascin-R in synapses of the adult rat hippocampus. J Neurobiol 2001;49:142–158.
31. Staubli U, Chun D, Lynch G. Time-dependent reversal of long-term potentiation by an integrin antagonist. J Neurosci 1998;18: 3460–3469.
32. Pagenstecher A, Stalder AK, Kincaid CL, *et al.* Differential expression of matrix metalloproteinase and tissue inhibitor of matrix metalloproteinase genes in the mouse central nervous system in normal and inflammatory states. Am J Pathol 1998;152:729–741.
33. Jaworski DM, Fager N. Regulation of tissue inhibitor of metalloproteinase-3 (Timp-3) mRNA expression during rat CNS development. J Neurosci Res 2000;61:396–408.
34. Li Z, Clarke MP, Barker MD, *et al.* TIMP3 mutation in Sorsby's fundus dystrophy: molecular insights. Expert Rev Mol Med 2005;7:1–15.

35. Langton KP, McKie N, Curtis A, *et al.* A novel tissue inhibitor of metalloproteinases-3 mutation reveals a common molecular phenotype in Sorsby's fundus dystrophy. J Biol Chem 2000;275:27027–27031.
36. Fariss RN, Apte SS, Luthert PJ, *et al.* Accumulation of tissue inhibitor of metalloproteinases-3 in human eyes with Sorsby's fundus dystrophy or retinitis pigmentosa. Br J Ophthalmol 1998;82:1329–1334.
37. Fedak PW, Smookler DS, Kassiri Z, *et al.* TIMP-3 deficiency leads to dilated cardiomyopathy. Circulation 2004;110:2401–2409.
38. Leco KJ, Waterhouse P, Sanchez OH, *et al.* Spontaneous air space enlargement in the lungs of mice lacking tissue inhibitor of metalloproteinases-3 (TIMP-3). J Clin Invest 2001;108: 817–829.

原　著

若年女性において飽和脂肪酸と野菜の1日摂取量はインスリン抵抗性と相関する

本田　まり[*1]　伊達ちぐさ[*1,*2]　呉　　斌[*1]　鈴木　一永[*1,*2]
福尾　恵介[*1,*2]　鹿住　　敏[*1,*2]

要約：18～22歳の女性85人においてインスリン抵抗性(イ抵抗性)と食事因子の関連を検討した．イ抵抗性はHOMA-IRで，体組成はDXAで，食事調査は7日間の秤量食事記録で評価した．HOMA-IR 2.5以上(対象の14%)はHOMA-IR 1.6未満と比べて，エネルギー，炭水化物，脂質，飽和脂肪酸(SFA)，穀類の1日摂取量が多かった．体脂肪量，レプチン，PAI-1，アディポネクチンとすべての栄養素を説明変数とした多変量解析では，体脂肪量(β=0.0001)，SFA摂取量(β=0.065)，βカロテン当量(β=−0.0002)が独立してHOMA-IRと相関した．食品群で同様に解析すると体脂肪量(β=0.0001)，乳類(β=0.003)，野菜類(β=−0.003)がHOMA-IRの規定因子であった．若年女性におけるイ抵抗性低減のためにはSFA(乳類)の過剰に注意し，野菜類の摂取を推奨する必要性が示唆された．

Key words：①若年女性　②インスリン抵抗性　③飽和脂肪酸　④野菜　⑤βカロテン
〔糖尿病52(4)：271～278, 2009〕

緒　言

肥満，2型糖尿病は今や中高年のみならず若年者にもみられる．インスリン抵抗性は肥満，2型糖尿病，脂質異常症，高血圧などの動脈硬化性疾患，さらにはメタボリックシンドロームの成因的基盤として重要である[1,2]．インスリン抵抗性の成因として内臓脂肪の蓄積に焦点をあてた研究が注目を集めているが，インスリン抵抗性に対する食事因子の詳細に関する報告は本邦では少なく[3]，若年者においてはほとんどみられない．本研究は若年女性におけるインスリン抵抗性と，摂取栄養素や摂取食品群の食事因子との関連について検討した．

方　法

武庫川女子大学生活環境学部食物栄養学科の学生101人を対象に，食事調査と血液生化学検査および体組成検査を行った．本研究の実施にあたって武庫川女子大学の倫理委員会の承認を得，また，すべての研究参加者から書面による参加の同意を得た．

血液生化学検査は食事調査から2週間以内に実施し，一夜絶食後，午前9時から10時半の間に肘静脈から採血を行い，空腹時血糖(FPG)，空腹時インスリン(FIRI：ELISA法，アボットジャパン)，HbA1c，レプチン(RIA法，LINCO社)，アディポネクチン(ELISA法，大塚製薬)，Plasminogen activator inhibitor-1(PAI-1)を測定した．体組成検査は二重エネルギー放射線吸収法(DXA：Hologic QDR-2000)を用いて測定した．インスリン抵抗性は空腹時血糖値と空腹時インスリン濃度から算出したHOMA-IR(Homeostasis model assessment insulin resistance index)を指標として用い，HOMA-IR 1.6以下を正常，2.5以上をインスリン抵抗性とした[4]．

食事調査は，すべての曜日を含んだ7日間の秤量食事記録をもとに行った[5]．実施前に説明会を行い，資料として，①食事調査協力に関する説明書，②食事内容記録方法の説明書，③自動秤1台(タニタ)，④食品

[*1] 武庫川女子大学生活習慣病オープン・リサーチ・センター(〒663-8558　兵庫県西宮市池開町6-46)
[*2] 武庫川女子大学生活環境学部食物栄養学科(〒663-8558　兵庫県西宮市池開町6-46)
連絡先：本田まり(〒513-8505　三重県鈴鹿市国府町112-1　鈴鹿回生病院)

受付日：2008年3月17日
採択日：2009年1月26日

Table 1 Anthropometric and bioclinical subject profiles

Age(years)	20.2±1.2
Body mass index(kg/m^2)	20.5±2.2
Body fat percent(%)	29.4±5.4
Body fat mass(kg)	15.4±4.5
Body lean mass(kg)	33.7±3.1
Fasting plasma glucose(mg/dl)	85.6±7.2
Fasting plasma insulin(μU/ml)	6.9±4.3
Hemoglobin A1c(%)	4.7±0.3
HOMA-IR	1.5±1.0
Leptin(ng/ml)	9.5±4.1
Adiponectin(μg/ml)	10.9±3.9
Plasminogen activator inhibitor-1(ng/ml)	17.5±8.5

Mean±SD. n=85. HOMA-IR: homeostasis model assessment of insulin resistance

重量の目安本(写真集)，⑤食品立体モデル(76品目)，⑥食事記録手帳，⑦身体状況に関する質問票，⑧歩数計，を配布した．食事の分析は，7日間の食事記録から1日当たり平均の摂取食品群と摂取栄養素を分析した．摂取栄養素の算出は，五訂日本食品成分表[6]に記載されている食品中の栄養素含有量を用い，摂取食品重量当たりの各栄養素の含有量を算出し，それらを総和して1日当たりの摂取量を算出した．栄養素の分析項目は，エネルギー，炭水化物，蛋白質(動物性，植物性)，脂質(動物性，植物性)，飽和脂肪酸(以下SFA)，一価不飽和脂肪酸(以下MUFA)，多価不飽和脂肪酸(以下PUFA)，ビタミンおよびミネラルを分析した．このほか，エネルギー密度(1日当たり摂取エネルギーを1日当たり摂取食品の総重量で除した値)，摂取エネルギーに対する3大栄養素の各エネルギー比率，動物性蛋白比，動物性脂質比，SFAエネルギー比(摂取エネルギーに対するSFAエネルギーの割合，以下MUFA，PUFAについても同様)，MUFAエネルギー比，PUFAエネルギー比，P/S(SFAに対するPUFAの割合)についても検討した．なお，評価可能な食事調査の回答は85人から得られた．

解析には統計ソフトSPSS15.0 for Windowsを使用した．HOMA-IRと食事因子の相関はSpearmanの順位相関係数，次いで多変量解析としてStepwise回帰分析を行った．HOMA-IRで3分類した群間の比較には分散分析を行い，体脂肪率で補正した．危険率5%未満を統計学的有意とし，結果は平均値±標準偏差または標準誤差で示した．

結　果

対象の平均年齢は20.2±1.2歳，平均BMIは20.5±2.2 kg/m^{2}であったが，DXAによる体脂肪率の平均は29.4±5.4%であった(Table 1)．空腹時血糖をはじめとした糖・インスリン代謝に異常はみられなかった．なお，食事調査の回答が得られなかった16人と得られた85人の間で体組成と血液生化学検査の成績に差はみられなかった．

1日当たり平均の食物摂取状況を，平成16年の国民栄養調査[7]における20歳台女性のデータと比較すると(Table 2)，摂取エネルギーは約90 kcal少なかった．脂質エネルギー比は日本人の摂取基準における目標量[8]の範囲内となる29.2%であった．また，豆類，野菜類，魚介類，肉類の摂取は少なく，乳類，菓子類，嗜好飲料類は多い傾向にあった．

HOMA-IRは栄養素では脂質，SFA，MUFAの摂取量との間に正の相関がみられた(Table 3, Fig. 1)．エネルギー比でみると，SFAエネルギー比はHOMA-IRと正に相関したが，脂質エネルギー比およびMUFAエネルギー比はHOMA-IRと相関しなかった．食品群では豆類と野菜類がHOMA-IRと負に相関した(Table 3, Fig. 1)．

85人中12人(14%)にHOMA-IR 2.5以上のインスリン抵抗性が認められた．一方，HOMA-IR 1.6以下の正常群は66%であった．インスリン抵抗性群の平均の体脂肪率は33.6%と高値であったため，体脂肪率で補正した後に比較すると(Table 4)，正常群と比べてインスリン抵抗性群は，BMI，PAI-1が有意に高かった．また，1日摂取エネルギー，炭水化物，脂質，SFA，MUFA，穀類，乳類の摂取量とSFAエネルギー比が有意に高値であった．

HOMA-IRを目的変数とした多変量解析の結果は(Table 5)，体脂肪量，レプチン，PAI-1，アディポネクチンと栄養素および食品群の全項目を説明変数としたモデル1では，体脂肪量(正)とSFA(正)，野菜類(負)がHOMA-IRを規定する独立因子であり，その寄与率は26%であった．体脂肪量，レプチン，PAI-1，アディポネクチンと栄養素の全項目を説明変数としたモデル2では，体脂肪量(正)とSFA(正)，βカロテン当量(負)がHOMA-IRの規定因子であり，その寄与率は25%であった．体脂肪量，レプチン，PAI-1，アディポネクチンと食品群の全項目を説明変数としたモデル3では，体脂肪量(正)，乳類(正)，野菜類(負)が規定因子であり，その寄与率は27%であった．

Tableには示していないが，SFAは乳類($r=0.53$, $p<0.01$)，肉類($r=0.44$, $p<0.01$)，油脂類($r=0.41$, $p<0.01$)と相関した．SFAを目的変数とした多変量解析では，乳類(正)がSFAの最大の規定因子であった(寄与率24%)．このほか，肉類，菓子類，穀類，油脂類が規定因子としてみられた(すべて正，寄与率

Table 2 Daily dietary intake in 85 young women

	Mean±SD	References*
Nutrients		
Energy (kcal)	1,568±336	1,659
Energy density (kcal/g)	0.95±0.22	0.92
Carbohydrates (g)	215.2±49.0	223.5
Protein (g)	55.3±12.0	62.2
Fat (g)	51.2±14.0	53.5
Saturated fatty acid (g)	14.0±4.2	—
Monounsaturated fatty acid (g)	17.6±5.2	—
Polyunsaturated fatty acid (g)	11.0±3.4	—
Carbohydrate (% energy)	54.9±4.6	56.1
Protein (% energy)	14.2±1.8	15.2
Fat (% energy)	29.2±4.3	28.7
Saturated fatty acid (% energy)	8.0±1.5	—
Monounsaturated fatty acid (% energy)	10.0±1.8	—
Polyunsaturated fatty acid/Saturated fatty acid	0.8±1.0	—
Foods		
Grain (g)	336.0±104.4	376.0
Sugar and/or sweeteners (g)	5.4±3.4	5.9
Pulses (g)	32.7±31.1	49.7
Vegetables (g)	173.0±80.4	223.0
Fruit (g)	90.8±85.1	83.1
Fish and shellfish (g)	38.3±25.2	63.5
Meat (g)	66.9±34.2	84.9
Milk and/or dairy products (g)	149.9±99.4	96.8
Oil and fat (g)	11.3±4.9	12.0
Confections (g)	56.5±37.8	28.9
Preferred beverages (g)	602.6±318.0	473.7

*References were data on women aged 20 to 29 years in the 2004 National Nutrition Survey in Japan

Table 3 Spearman's correlations of HOMA-IR with dietary factors

Nutrient	r	Food	r
Energy (kcal)	0.16	Grain	0.14
Energy density (kcal/g)	0.12	Sugar and/or sweetener	0.18
Carbohydrates (g)	0.11	Pulses	−0.25*
Protein (g)	0.06	Vegetables	−0.22*
Fatty acid (g)	0.24*	Fruit	−0.04
Saturated (g)	0.25*	Fish and shellfish	0.01
Monounsaturated (g)	0.26*	Meat	0.08
Polyunsaturated (g)	0.19	Eggs	−0.05
Carbohydrate (% energy)	−0.10	Milk and/or dairy products	0.16
Protein (% energy)	−0.16	Oil and fat	0.02
Fat (% energy)	0.17	Confections	0.03
Saturated fatty acid (% energy)	0.23*	Preferred beverages	0.10
Beta carotene potency (μg)	−0.17	Seasonings	−0.20

*: $p<0.05$. n = 85